Report Vehicle Controls

Francesco Mecatti
299822@studenti.unimore.it

Exercise 1: Longitudinal Control

In this exercise, I experimented with PID tuning and anti-windup techniques. As required by the assignment, the lateral control is kept disabled throughout the tuning phase of the longitudinal PID and the steering angle has been fixed to zero, resulting in the vehicle traveling perfectly straight for 500 meters, as shown by fig. 1.

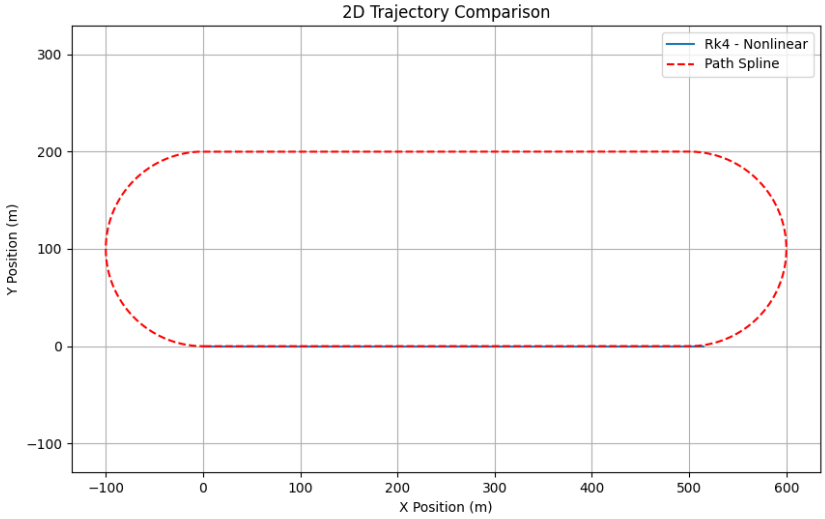

Figure 1: Exercise 1 trajectory

Gain values are found through a trial and error process: starting from the coefficient K_p, then moving to the coefficient K_i, and eventually up to the coefficient K_d.

What can be observed during the tuning process is that just the proportional component alone is not enough to lead the velocity to its target. What's more, the greater K_p the lower the rise time, but the higher the steady-state error. The sweet spot is hence found as a trade-off of rise speed and steady-state error.

By adding the integral component, I ensured the target is reached at steady-state, however, an oscillatory behavior is introduced; therefore I had to balance out the two effects once again. The instability of a PI controller for longitudinal velocity can be seen primarily with geometric controllers (MPC suffers less from this thanks to its predictive capabilities) at the moment in which the vehicle performs a turn - i.e. when its trajectory is sort of perturbed after the straight line. Figure 2 shows this instability when tracking the reference path at 23m/s over a single lap with the Pure Pursuit (PP) lateral controller.

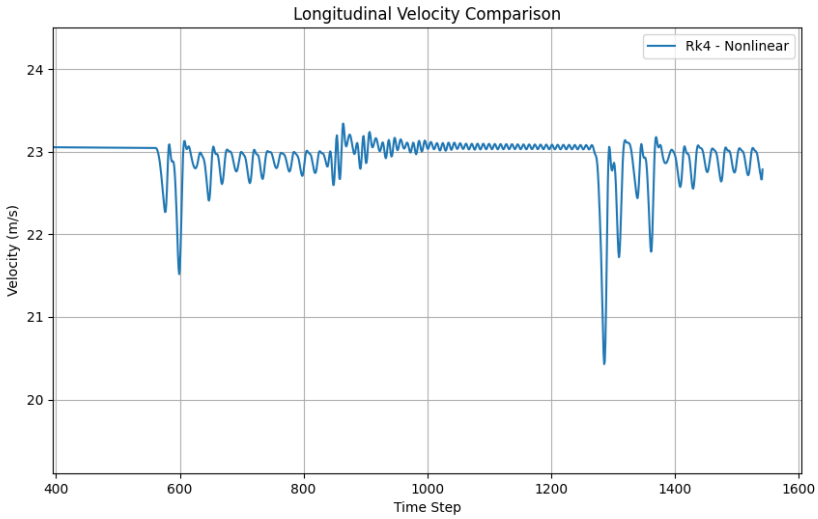

Figure 2: PI control instability

Lastly, the derivative component contributes to the system stability, reducing just-mentioned oscillations. As in the previous cases, an excessive gain leads to high-frequency oscillations, which are clearly undesired since they could degrade the performance of the system.

The tuning process results in the following coefficients: $(K_p, K_i, K_d) = (2, 0.04, 0.1)$. Figure 3 and fig. 4 illustrate the vehicle's longitudinal velocity plot with, respectively, a target of 15m/s and 25m/s. In these figures, there is no overshoot, which means that the system is critically damped. The rise time, defined as the time required by the system to rise to the 90% of the target, is 150 steps (equal to 7.5s) in the first scenario and roughly 250 steps (12.5 s) in the second one. The settling time is a little higher, approximately equal to, respectively, 200 and 300 steps.

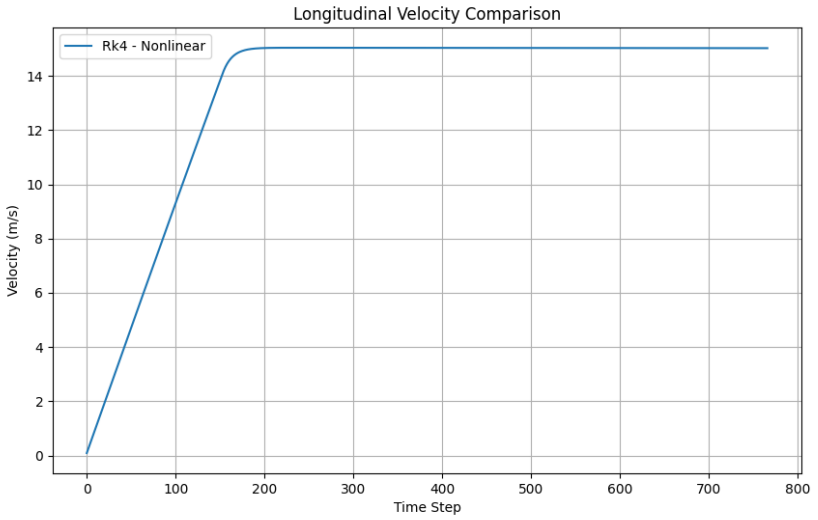

Figure 3: Longitudinal velocity @ 15m/s

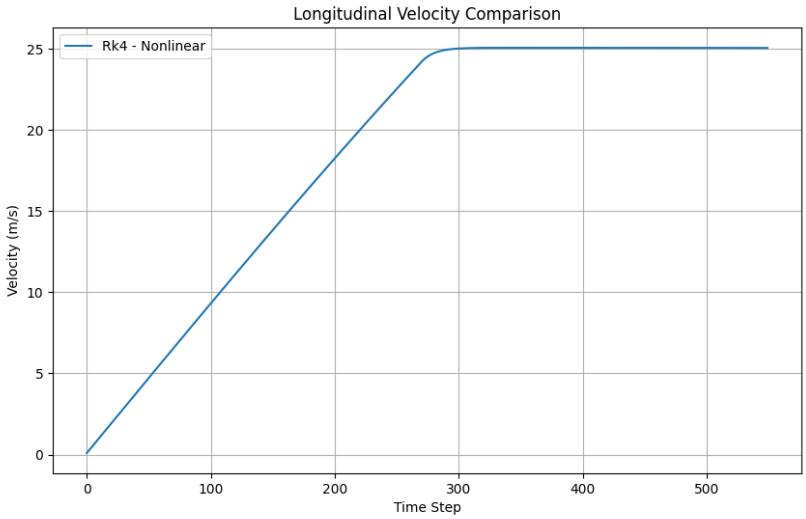

Figure 4: Longitudinal velocity @ 25m/s

The steady-state error is around zero, as proved by fig. 5 at 25m/s; the same applies to a speed of 15m/s. Additional figures, such as the controller output acceleration and the longitudinal velocity error at 15m/s can be found in the *figures* folder.

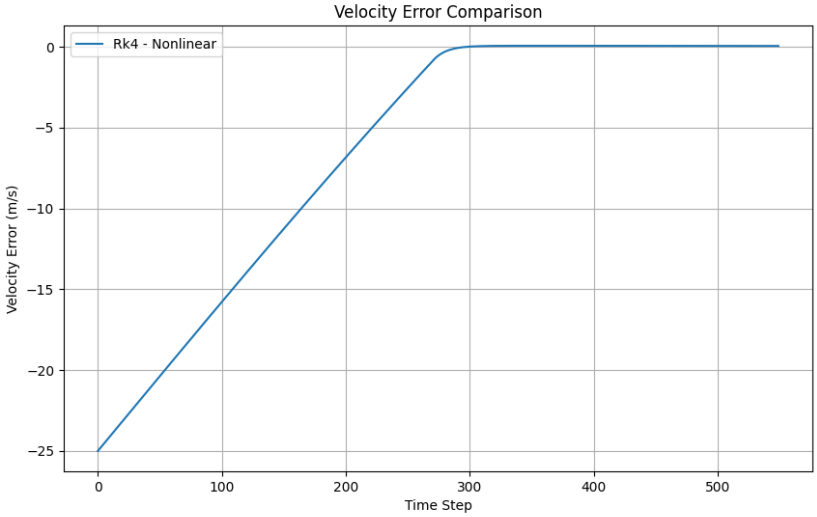

Figure 5: Velocity error @ 25m/s

Exercise 2: Low-Speed Lateral Control

In this exercise, the Pure Pursuit (PP) and Stanley controllers have been tested. The performance metric used in this and in the following exercise to understand whether a formula change or parameter tweaking resulted in a better or worse overall performance is the sum of the lateral errors (euclidean distance between ego vehicle position and target point) at each time step. This value provides a summarized picture of whether a change led to an improvement or not.

To ensure that the simulation was long enough to complete a single lap of the track, a strategy based on the number of times the right semi-plane is encountered has been implemented. Basically, a 2 meters wide dead band around $x = 0$ has been defined; its boundaries are therefore $x = -1$ (left boundary) and $x = 2$ (right boundary). These two boundaries split the x-axis into 3 regions: left semi-plane, dead band, and right semi-plane. The termination condition is triggered when the right semi-plane is encountered for the second time, hence as soon as the $x = 2$ boundary is crossed after a visit on the left semi-plane.

Moving on to the controllers, both PP and Stanley have been successfully tuned and used to track the reference path, at both 10m/s and 20m/s, as shown by fig. 6 and fig. 7 (figures of the lateral error at 10m/s are not included, as the error is constantly nearly zero, but can be found in the attached *figures* folder). These two plots show that the lateral error is consistently below 1m, thus respecting the "tolerance" imposed by the assignment.

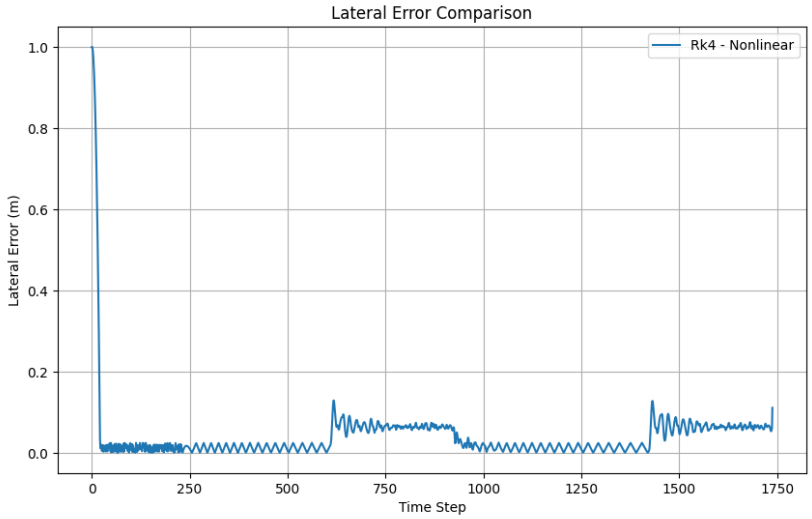

Figure 6: PP lateral error @ 20m/s

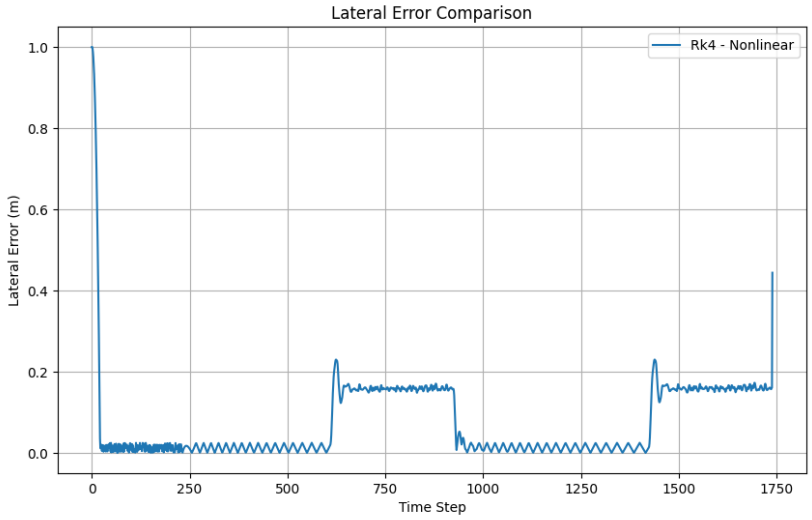

Figure 7: Stanley lateral error @ 20m/s

When it comes to the controllers' formulation, the original code has been modified, in order to move the CoG to the right axle for each of them: the rear axle for PP and the front axle for Stanley. The formulae used to perform the translation are, respectively, $CoG_{PP} = \begin{bmatrix} x - L_r \cos(yaw) \\ y - L_r \sin(yaw) \end{bmatrix}$ and $CoG_{Stanley} = \begin{bmatrix} x + L_f \cos(yaw) \\ y + L_f \sin(yaw) \end{bmatrix}$.

It is also worth mentioning that the original PP formula has been extended to dynamically adjust the look-ahead distance according to the speed of the vehicle:

```
bounded_cur = max(1e-2, abs(path_spline.calc_curvature(path_spline.cur_s)))
Lf = base_look_ahead + k_v_pp * sim.vx + k_c_pp / bounded_cur
```

The formula is parametrized wrt `k_v_pp` (set to 0.05 in my script), namely the velocity gain, and wrt `k_c_pp` (set to 0.0001), that is, the curvature gain. It can also be seen how the curvature at the given point is lower

bounded by a small real number (0.01), to prevent division by zero to occur. Lastly, the `base_look_ahead` parameter acts as an offset for the look-ahead distance and has been set to 0.5m in the script.

Exercise 3: High-Speed Lateral Control

In this exercise, PP and Stanley controllers have been pushed to their limit, which proved to be 25 m/s without relaxing the original constraints. It follows that the MPC controller has been tested to track the path at higher speeds, with kinematic, linear ST and nonlinear ST models, reaching a maximum speed of 29 m/s with the linear ST model (without relaxing the original constraints).

The reason why geometric controllers fail at such high speeds can be justified with their instability, especially visible in the oscillatory behavior of the steer. Figure 8 shows the steering value over time for the PP controller at 20m/s (from exercise 2) and has been included as a reference; fig. 9 shows the same plot at a speed of 25m/s (so +5m/s) and demonstrates how the peak compensation varies from 0.15 rad to 0.4 rad, meaning an increase factor of 2.7. For reference, increasing the speed from 10m/s to 20m/s makes the peak compensation vary from 0.06 to 0.15 (just a factor of 2.5); meaning, this peak compensation value is not growing linearly with the speed: a small increase in the target speed could cause a severe growth in steer oscillations.

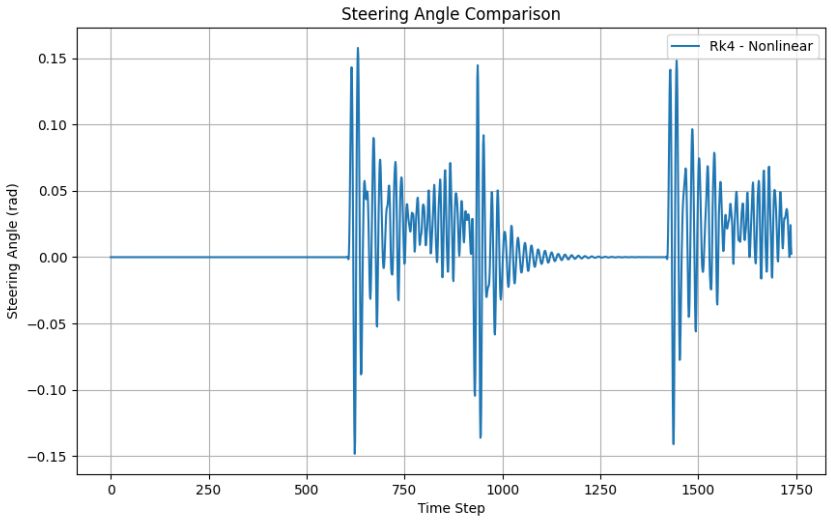

Figure 8: PP output steer @ 20m/s

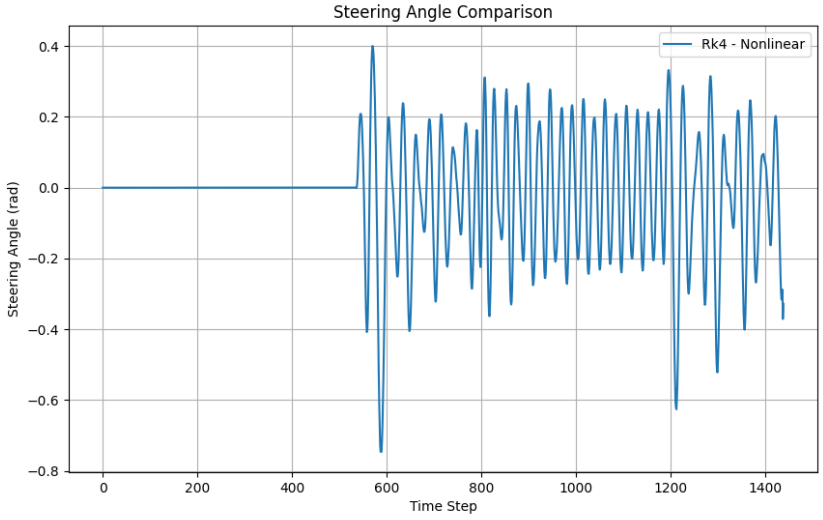

Figure 9: PP output steer @ 25m/s

Instead, a predictive controller such as MPC suffers much less from this problem, as illustrated by the plot fig. 9. Not only is the order of magnitude at peaks 10 times smaller, but the shape of the output curve is also less aggressive. It follows that this controller, as opposed to the geometric ones, has a larger speed improvement margin.

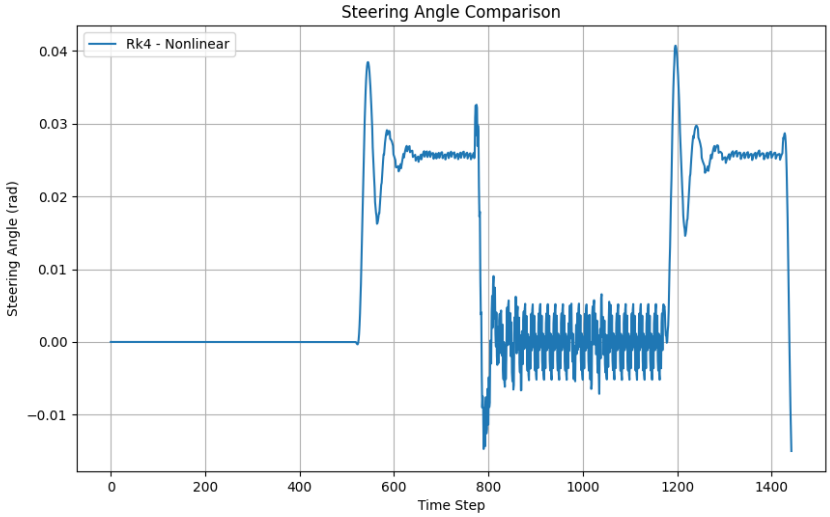

Figure 10: MPC w/ linear ST model output steer @ 25m/s

In addition to that, the choice of the lateral controller also has an impact on the longitudinal controller; in fact, the performance of the lateral controller goes hand in hand with the performance of the longitudinal controller, and vice versa. It can be proved that an aggressive steering strategy leads to the instability of the longitudinal PID, due to sudden steering adjustments that the PID struggles to follow. By comparing fig. 11 with fig. 12 the just mentioned side/cross effects are clearly visible. A potential solution is the use of a combined controller, able to take into account even the side effects they have on each other.

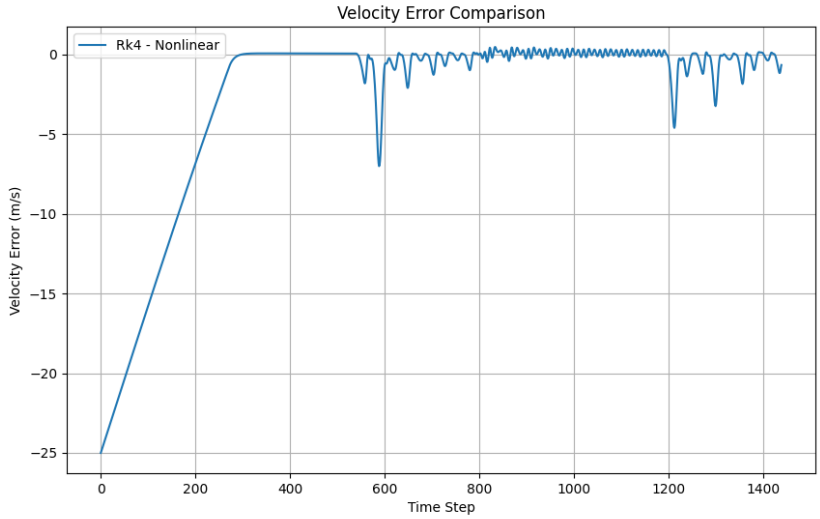

Figure 11: PP longitudinal velocity error @ 25m/s

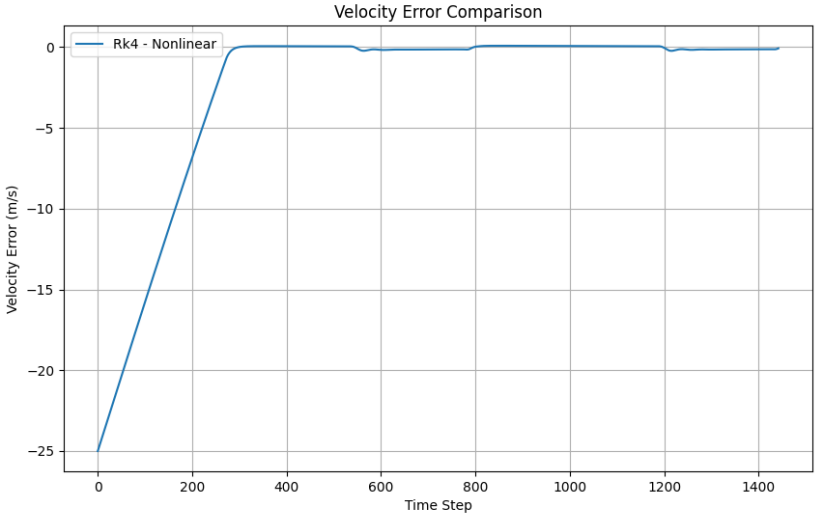

Figure 12: MPC w/ linear ST model velocity error @ 25m/s

Lastly, figures from Figure 13 to Figure 15 show the lateral error of the three controllers at their maximum speed, proving that the constraint on the lateral error is respected. Reaching 29m/s with the MPC controller has been made possible by the replacement of the original kinematic model with a linear single track model (also the nonlinear model has been tested but underperforms the linear one), along with a good tuning of the gains. In particular, the rate-of-change penalty gain has been made dependent on the speed of the vehicle:

```
J += mtimes(Us.T,Us) * (1000.0 + 100 * state.vx)
```

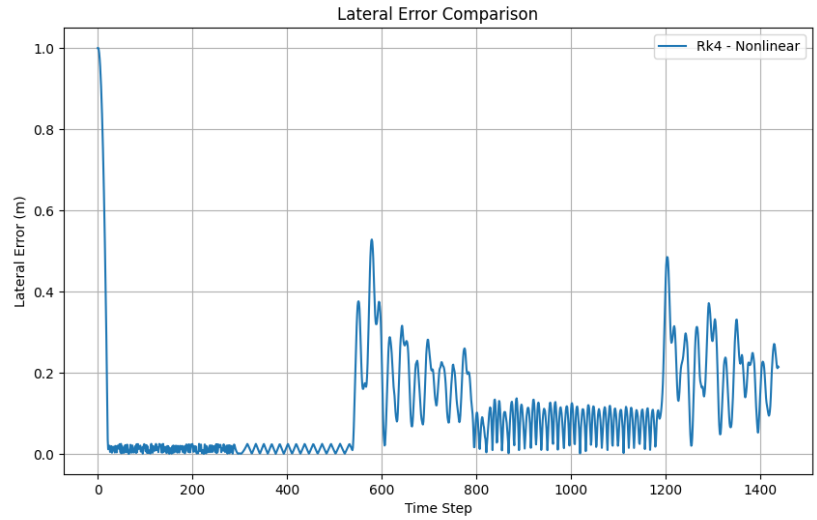

Figure 13: PP lateral error @ 25m/s

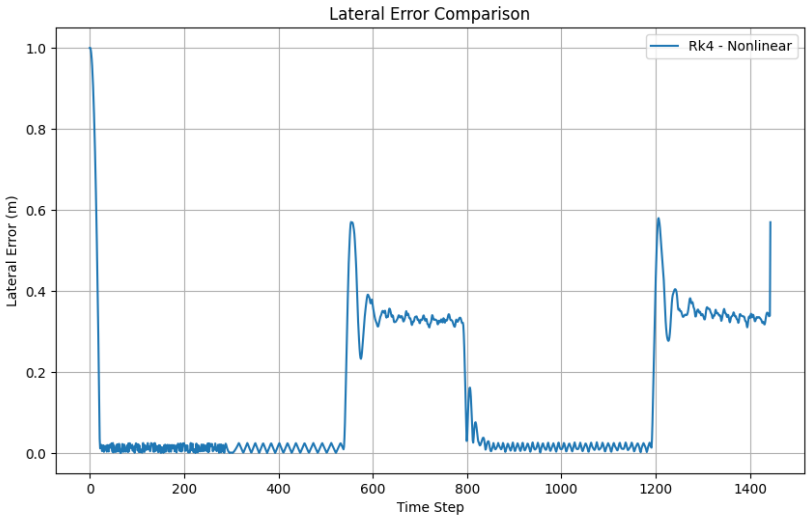

Figure 14: Stanley lateral error @ 25m/s

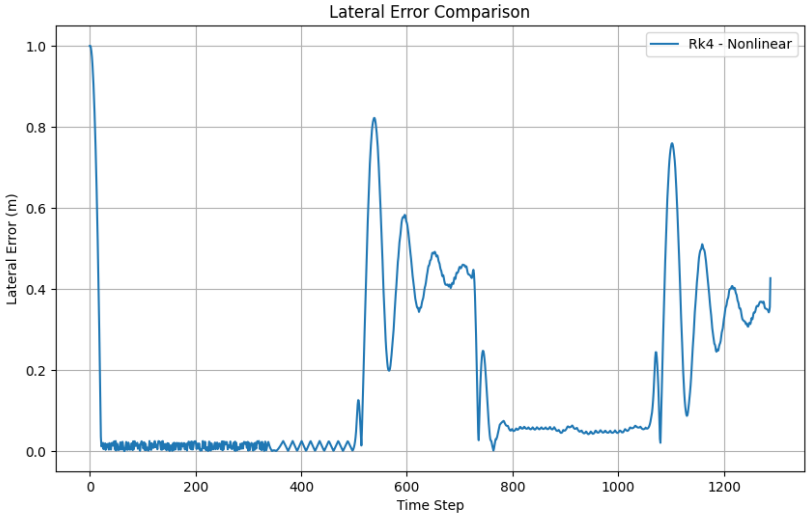

Figure 15: MPC w/ linear ST model lateral error @ 29m/s